Regenerative Therapy 21 (2022) 62–72

Contents lists available at ScienceDirect

Regenerative Therapy

journal homepage: http://www.elsevier.com/locate/reth

Original Article

Transplantation of human cells into Interleukin-2 receptor gamma gene knockout pigs under several conditions

Koki Hasegawa [a, 1], Kazuaki Nakano [b, c, 1], Masaki Nagaya [c, *, 1], Masahito Watanabe [b, c], Ayuko Uchikura [a, c], Hitomi Matsunari [a, c], Kazuhiro Umeyama [b, c], Eiji Kobayashi [d], Hiroshi Nagashima [a, c, **]

[a] Laboratory of Developmental Engineering, Department of Life Sciences, School of Agriculture, Meiji University, 1-1-1 Higashimita, Tama-ku, Kawasaki 214-8571, Japan
[b] PorMedTec Co. Ltd., 2-3227 MIta, Tama-ku, Kawasaki, Kanagawa, 214-0034, Japan
[c] Meiji University International Institute for Bio-Resource Research, 1-1-1 Higashimita, Tama-ku, Kawasaki 214-8571, Japan
[d] Department of Kidney Regenerative Medicine, The Jikei University School of Medicine - Tokyo, Japan

ARTICLE INFO

Article history:
Received 21 February 2022
Received in revised form
22 April 2022
Accepted 25 May 2022

Keywords:
Interleukin-2 receptor gamma
SCID
Pig
Xenotransplantation

ABSTRACT

Introduction: Previously, we performed gene knockout (KO) of interleukin-2 receptor gamma (*IL2RG*) in porcine fetal fibroblasts using zinc finger nuclease-encoding mRNAs, subsequently generating *IL2RG* KO pigs using these cells through somatic cell nuclear transfer. The *IL2RG* KO pigs lacked a thymus and were deficient in T lymphocytes and natural killer cells, similar to human X-linked severe combined immunodeficiency (SCID) patients. The present study aimed to evaluate whether pigs can support the growth of xenografted human cells and have the potential to be an effective animal model.
Methods: The *IL2RG* $X^{KO}Y$ pigs used in this study were obtained by mating *IL2RG* $X^{KO}X$ females with wild-type boars. This permitted the routine production of *IL2RG* KO pigs via natural breeding without complicated somatic cell cloning procedures; therefore, a sufficient number of pigs could be prepared. We transplanted human HeLa S3 cells expressing the tandem dimer tomato into the ears and pancreas of *IL2RG* KO pigs. Additionally, a newly developed method for the aseptic rearing of SCID pigs was used in case of necessity.
Results: Tumors from the transplanted cells quickly developed in all pigs and were verified by histology and immunohistochemistry. We also transplanted these cells into the pancreas of designated pathogen-free pigs housed in novel biocontainment facilities, and large tumors were confirmed.
Conclusions: *IL2RG* KO pigs have the potential to become useful animal models in a variety of translational biology fields.

1. Introduction

Pigs are large animals with similar anatomy and physiology to humans and are effective models for biomedical research [1–4]. The high sequence homology of pigs with human xenobiotic receptors may allow the accurate prediction of the pharmacodynamic and pharmacokinetic properties of drugs compared to rodents [5]. For surgical and clinical monitoring purposes, rodents are too small to be practical [6,7]. Thus, there is a demand for sophisticated pig animal models, which may improve the translation efficiency from preclinical to clinical studies.

IL2RG, the common gamma chain, is an indispensable subunit of functional receptor complexes for the following interleukins (ILs); IL-2, IL-4, IL-7, IL-9, IL-15, and IL-21 [8–14]. The common

Abbreviations: SCID, Severe combined immunodeficiency; KO, knock out pigs; WT, wild-type pigs; IL, Interleukin; *IL2RG*, interleukin-2 receptor gamma; SCNT, somatic cell nuclear transfer; NK cells, natural killer cells; OIDP, operational immunodeficient pig; ZFN, Zinc finger nuclease; XLGD, X-linked genetic diseases; DPF, designated pathogen-free; PCR, polymerase chain reaction; U-iR, uterectomy-isolated rearing; tdTomato, tandem dimer Tomato; SD, standard deviation.

* Corresponding author. Meiji University International Institute for Bio-Resource Research, 1-1-1 Higashimita Tama-ku Kawasaki, Kanagawa 214-8571, Japan. Tel./fax: +81 44-934-7824.
** Corresponding authors. Laboratory of Medical Bioengineering, Department of Life Sciences, School of Agriculture, Meiji University, 1-1-1 Higashimita Tama-ku Kawasaki, Kanagawa 214-8571, Japan. Tel./fax: +81 44-934-7824.
E-mail addresses: m2nagaya@meiji.ac.jp (M. Nagaya), hnagas@meiji.ac.jp (H. Nagashima).

Peer review under responsibility of the Japanese Society for Regenerative Medicine.

[1] KH, NK, and MN contributed equally to this work.

https://doi.org/10.1016/j.reth.2022.05.010

gamma chain plays a key role in the differentiation of T lymphocytes and natural killer (NK) cells [15,16]. The porcine common gamma chain gene, assigned to swine chromosome Xq13, comprises eight exons, spans approximately 3.7 kb and encodes a 368-amino acid polypeptide [13,15]. A mutation in the IL2RG gene induces a marked decrease or depletion of T and NK cells and loss of production of antibodies from B cells. This is seen in human X-linked SCID patients [17], which is a genetic disorder of the functions of major lymphocytes, such as B and T cell impairment [18,19].

SCID pigs arose spontaneously in a standard breeding program [20,21]. They were unable to produce antibodies, had atrophied lymph nodes, and lacked a thymus and B and T cells. In addition, SCID-like pigs are generated using genetically modified techniques. So far, Suzuki et al. [22] and our group [23] have disrupted the X-linked porcine gene encoding IL2RG and obtained SCID-like pigs through various strategies. Suzuki et al. targeted *IL2RG* in somatic cells via homologous recombination and used serial somatic cell nuclear transfer (SCNT). Subsequently, they performed further breeding to generate heterozygous *IL2RG*$^{+/-}$ females and *IL2RG*$^{-/Y}$ males. The males were athymic and had impaired immune cell production. Our group used the more efficient ZFN-encoding mRNA technology to knock out the IL2RG gene in porcine fetal fibroblasts. *IL2RG* KO pigs were generated using KO cells via SCNT. The pigs completely lacked a thymus and were deficient in T and NK cells. The use of ZFNs is promising for creating genetically engineered pigs [23–25]

Human xenotransplantation studies were not possible in pigs until the identification [20,21,26] or creation [22–25,27–30] of SCID-like pigs. SCID pigs have been reported to accept grafts of human melanoma (A375SM) and pancreatic carcinoma (PANC-1) cancer cell lines [20], OSPC-ARK1 primary ovarian cell lines [31], and human induced pluripotent stem (iPS) cells [32,33]. However, several issues are constantly raised in obtaining SCID-like pigs: 1. Additional cloning and breeding steps are required; 2. Pigs require 7 months to reach sexual maturity; 3. There is a high possibility of severe infection due to disruption of the immune system during rearing [25]; and 4. They often suffer from reproductive problems. Therefore, the establishment of an efficient reproductive system is key for acquiring *IL2RG* KO pigs. Previously, we showed that the valuable traits of *IL2RG* KO pigs can be maximized by generating unique chimeric boars composed of mutant and normal cells [25]. The chimeric boars exhibited a cured phenotype with fertility when carrying and transmitting the X-linked genetic disease (XLGD) genotype. Male-based breeding with wild-type (WT) female pigs permits the routine production of *IL2RG* KO pigs in a Mendelian fashion.

The present study aimed to evaluate whether the generated *IL2RG* KO pigs can host and support the growth of xenografted human cells under several conditions. Currently, we have developed a feasible and economical method to produce designated pathogen-free (DPF) pigs, which involves a uterectomy procedure on a full-term sow, the recovery of fetuses from the uterus, and the rearing of neonatal piglets under aseptic conditions in specially designed isolator units [34]. We termed this method the uterectomy-isolated rearing (U-iR) method. Considering the vulnerability of *IL2RG* KO pigs to infection, the method was attempted for this study because it allows for long-term follow-up if the system is functional.

Recently, Itoh et al. [35] developed an immunodeficient pig model, the operational immunodeficient pig (OIDP), by surgically removing the thymus and spleen and creating a controlled immunosuppressive protocol with a combination of drugs commonly used in the clinical setting. This model allowed for the long-term accommodation of artificial human vascular grafts. Therefore, this study also comparatively investigated the differences between *IL2RG* KO pigs and OIDPs.

2. Materials and methods

2.1. Animals

All animal experiments performed in this study, including the creation of immunodeficient pigs, xenotransplantation, and the production of DPF pigs, were approved by the Institutional Animal Care and Use Committee of Meiji University (IACUC, IACUC15-0005, IACUC17-0006, IACUC18-0004, and MUIACUC2020-05). All experiments were performed in accordance with the relevant guidelines and regulations. All animals were maintained under conventional conditions in an air-conditioned room, bred, and observed daily by the animal husbandry personnel. All efforts were made to minimize suffering.

2.2. Production of IL2RG KO pigs

The *IL2RG* $X^{KO}Y$ pigs used in this study were obtained by mating *IL2RG* $X^{KO}X$ females with WT boars. We have previously produced an *IL2RG* $X^{KO}Y \leftrightarrow X^{WT}X^{WT}$ chimeric boar via blastocyst complementation with *IL2RG* $X^{KO}Y$ and WT cloned embryos [25] (Supplementary Fig. 1). This chimeric boar was used to breed WT females which could generate *IL2RG* $X^{KO}X$ progeny. *IL2RG* $X^{KO}X$ progeny (IL2RG mutation carriers) were bred for approximately 7–15 months before the first mating. *IL2RG* $X^{KO}Y$ pigs were surgically obtained from the uteri of pregnant females at 112 days of gestation using a previously reported procedure [36]. Briefly, the uterus of a pregnant female was exenterated and placed in an isolation chamber sterilized with 0.1% peracetic acid vapor. Piglets were removed from the uterus through an incision in the uterine wall and, once breathing spontaneously, were moved to a rearing isolator for artificial nursing.

2.3. Genotyping

Genotyping was performed as previously described [23]. Briefly, genomic DNA was extracted from a tail biopsy and/or the umbilical cord specimens of newborn piglets using a DNeasy Blood and Tissue Kit (Qiagen, Hilden, Germany). The target region of IL2RG was amplified from the cell clones by direct PCR using MightyAmp DNA polymerase (Takara Bio, Shiga, Japan) and the appropriate primers (5-ATACCCAGCTTTCGTCTCTGC and 5-TTCCAGAATTCTATACGACC). The PCR products were separated by agarose gel electrophoresis to determine whether they were WT, heterozygous (female carrier; *IL2RG* $^{+/-}$), or SCID (*IL2RG* $^{-/Y}$).

2.4. Production of DPF pigs using U-iR method

The DPF pigs were treated in different ways. Each excised uterus was transferred to an aseptic isolator (recovery unit) via a disinfecting tub filled with 0.05% peracetic acid, and fetuses were recovered from the uterus within 5 min. The piglets were then transferred to a second isolator unit (rearing unit, 1–5 piglets/unit) for artificial nursing with γ-irradiated milk substitute and kept in the novel biocontainment rearing unit (Supplementary Fig. 2) until the study was complete.

2.5. Microbiological testing

Swab samples from the body surface, oral mucosa, and feces of the pigs were obtained using the U-iR method, while samples from the internal surface of the rearing unit were collected weekly. The

samples were cultured on thioglycolate and potato dextrose agar and examined using a standard protocol developed and recommended by the Japanese Association for Laboratory Animal Science [37]. The samples were analyzed for sterility and the presence of viruses.

2.6. Production of different immunodeficient pigs

We prepared three different forms of immunodeficient pig in this study. The OIDP was produced as described by Itoh et al. [35], with some modifications. One male Large White/Landrace x Duroc pig (34 days after birth) was anesthetized by isoflurane inhalation. A midline incision was made in the ventral region of the neck and three lobes of the thymus were excised. Laparotomy was performed by making an incision in the middle of the abdomen to remove the spleen. Simultaneously, the upper portion of the stomach was exposed and a catheter (16 F, JMS hydrophilic Foley catheter, JMS) was inserted, after which the stomach and catheter insertion site were ligated and fixed (K302: K1). The second pig went through the same procedure, without a splenectomy (K303: K2) and the third pig underwent gastrostomy only (K304: K3). All three pigs underwent surgery 16 days before transplantation and were treated with immunosuppressive drugs according to the following protocol: Tacrolimus hydrate was administered at 0.5 mg/kg/day (Pfizer, New York, NY, USA); mycophenolate mofetil (MMF) was administered at 60 mg/kg/day (Pfizer); and prednisolone was administered at 20 mg/pig/day (Teva Takeda Pharma, Tokyo, Japan). All drugs were administered through the gastric tube 6 days before transplantation. The day of transplantation was defined as day 0. The blood tacrolimus and MMF concentrations were measured at SRL International, Inc., Japan, and the dose was adjusted so that the trough levels of these drugs could be measured.

2.7. Preparation of donor human cells

For human donor cells, we selected the human cervix carcinoma cell line HeLa S3 (National Institutes of Biomedical Innovation, Health, and Nutrition, Osaka, Japan) for this study and modified the cells to express the tandem dimer Tomato (tdTomato). HeLa S3 cells were grown in F12 medium with 10% FBS (Sigma–Aldrich, St. Louis, MO, USA) and antibiotic-antimycotic solution (Thermo Fisher Scientific) until 80% confluence and were passaged several times for preparation. The tdTomato expression vector used in the present study was prepared using our previously reported method [38]. The vector consisted of a chicken beta-actin promoter with a cytomegalovirus enhancer (CAG promoter), tdTomato cDNA, a rabbit beta-globin 3′-flanking sequence including a polyadenylation signal, and the puromycin N-acetyltransferase gene driven by the phosphoglycerate kinase promoter. For transfection, HeLa S3 cells were cultured to 70–90% confluence, washed twice with Dulbecco's phosphate-buffered saline, and collected after treatment with 0.05% trypsin-ethylenediaminetetraacetic acid (trypsin–EDTA, Life Technologies). The collected cells (6.0×10^5) were then resuspended in 60 μL of resuspension buffer supplied as part of a NeonTransfection System kit (Life Technologies) and 1.5 μg of the tdTomato expression vector was added. The cells were then electroporated under the following conditions: Pulse voltage, 1200 V; pulse width, 20 ms; pulse number, 2. After 48 h of electroporation, the cells were transferred to a medium containing 2.5 μg/mL puromycin. After 12 days in culture, puromycin-resistant cells were collected and a limiting dilution was performed to obtain single cell-derived clones. tdTomato-positive cells were grown to confluence and cryopreserved for later use as donor cells for transplantation.

2.8. Cell transplantation

For transplantation, the cells were brought to a concentration of 3×10^6 cells/0.2 mL or 1×10^5 cells/0.05 mL. The cells were placed on ice until immediately before the transplantation.

All pigs in the following experiment were anesthetized by administration of isoflurane gas vaporized into oxygen and delivered via a face mask. The transplanted cells were monitored for tumor development.

2.9. Experiments

2.9.1. Experiment 1: evaluation of transplanted human cells in IL2RG KO and WT pigs in conventional rearing

Seven *IL2RG* KO and six WT pigs were prepared, and donor cells were transplanted subcutaneously into one or both ears one day after birth. Two *IL2RG* KO pigs and three WT pigs received transplants into both ears, while all others received transplants in one ear only. Donor cells (3×10^6) were suspended in 200 μL phosphate-buffered saline (PBS) for each transplant.

2.9.2. Experiment 2: evaluation of human cells transplanted into the pancreas of DPF IL2RG KO pigs housed in novel biocontainment facilities

Two 7-day-old *IL2RG* KO pigs underwent laparotomy in an isolator unit under sterile conditions. Pigs were transplanted with 1×10^5 cells in 50 μL of PBS-cell suspension into the tail of the pancreas.

2.9.3. Experiment 3: comparison between the IL2RG KO pigs and other immunodeficient models

This study also comparatively investigated the differences between *IL2RG* KO pigs and other immunodeficient models. Three immunodeficient pigs were produced through three different operations including OIDP 16 days before transplantation. The day of transplantation was defined as day 0. Cells were transplanted into both ears in the same manner as in Experiment 1 and these pigs were reared in conventional housing.

2.10. Size of the tumor at the transplanted site

First, the tumor from the transplanted cells was verified to determine whether it emitted red tdTomato signals using a fluorescent lamp and filter. Once confirmed, the short and long diameters of the tumor at the transplant site were measured. Tumors were visually inspected daily for tumor growth in all experiments. Slide calipers were used to measure the tumor volume and calculated using the following formula: Short diameter^2 × long diameter/2.

2.11. Histology

Samples from each transplantation site were collected at every time point. The tissue samples were immediately fixed in 4% paraformaldehyde, embedded in paraffin, and sectioned at a thickness of 4 μm. Hematoxylin-eosin (HE) staining and analysis were performed to establish the presence of tumor architecture, following previously described immunohistochemical methods [39,40]. Briefly, after deparaffinization and blocking, sections were incubated with diluted primary antibodies overnight at 4 °C. The following primary antibodies were used: Common lymphocyte marker [35] rabbit anti-CD45 (Abcam plc, Cambridge, UK), T lymphocyte marker [35] anti-CD3 (DAKO, Santa Clara, CA, USA), B lymphocyte marker [35] anti-CD20 (Thermo Fisher Scientific), NK cell marker [41] anti-CD56 (LSBio, Seattle, WA), monocyte/

macrophage lineage and dendritic cell marker [42] anti-Iba1 (Wako Pure Industries), cytotoxic T cell and NK cell marker [43,44] anti-granzyme B (Abcam plc), and major histocompatibility complex class II molecule marker [45,46] anti-HLA-DR (DAKO). Horseradish peroxidase (Rabbit/Mouse, DAKO) was used as the secondary antibody. A liquid DAB + Substrate Chromogen System (DAKO) was used as the substrate for colorization. The negative controls included sections incubated with secondary antibodies only. The number of CD45+ cells 1 week after transplantation was quantified using the Hybrid Cell Count Module (H4A; Keyence, Osaka, Japan). To evaluate the CD45+ cells, we counted them in three randomly selected areas of six samples from the transplant sites of two different *IL2RG* KO and WT pigs (four pigs in total). The mean value for each lobe was calculated on every day of assessment. The sections were examined under an all-in-one fluorescence microscope (BZ-X800; Keyence, Osaka, Japan) and the built-in software was used for data analysis (BZ-H4A; Keyence).

2.12. Statistical analyses

Statistical analyses were performed with SPSS software (version 26; IBM Corporation, New York, USA). Data were averaged and expressed as mean ± standard deviation (SD). Unpaired Student's t-tests, repeated measures one-way analysis of variance, and Fisher's protected least significant difference tests were used to compare groups. Results with p values of less than 0.05 compared with the WT were considered statistically significant.

3. Results

3.1. Repetition of phenotypic symptoms in offspring

Four *IL2RG* $X^{KO}X$ females grew into healthy fertile adults. No deaths occurred during rearing. From four females, 13 *IL2RG* KO males were obtained from 35 siblings (37.1%). They harbored the same *IL2RG* mutation as the nuclear donor cells.

3.2. Pig observations and development of tumors

3.2.1. Experiment 1: evaluation of transplanted human cells in IL2RG KO and WT pigs in conventional rearing

After transplantation, both *IL2RG* KO and WT pigs exhibited normal growth and development over time (Fig. 1A). In both groups, the transplanted cells were chronologically followed (Fig. 1B and C). In *IL2RG* KO pigs, transplanted cells were identified visually and by palpation one week after transplantation. The transplanted cells developed into tumors with small, firm, raised, and elongated masses (Fig. 1B).

At 3 weeks, the pigs were euthanized, and the tumors in the ears were dissected. Broad photographs of the tumors were taken (Fig. 1D, left) and it was confirmed that the cells were strongly red (Fig. 1D, right). The tumors were substantially larger than those at 1 week after transplantation, measuring in at 6930.3 ± 918.0 mm^3 (Fig. 1B and E).

In WT pigs, 1 week after transplantation, the transplanted cells were visually identified as tumors, but the size was smaller; *IL2RG* KO 1135.4 ± 556.5 mm^3 vs WT 528.3 ± 250.8 mm^3 ($p < 0.05$; Fig. 1C and E). No obvious tumors were observed at 2 weeks after transplantation (Fig. 1C and E).

Histology and immunohistochemistry revealed the presence of transplanted cells in all transplanted sites in *IL2RG* KO pigs 1 week after transplantation (Fig. 2A and A′). The tumors were well demarcated and formed nests (Fig. 2A, left). The transplanted cells clonally expanded at the transplanted site (Fig. 2A, right) and scarce CD45+ cells were confirmed (Fig. 2A).

In WT pigs, 1 week after transplantation, transplanted cells were also confirmed (Fig. 2B). Within the subcutis of the ear, moderately demarcated tumors were observed (Fig. 2B, left) but they lacked the same density as the tumors in the *IL2RG* KO pigs (Fig. 2B, right). The number of infiltrating CD45+ cells in the tumor area was confirmed as 46.7 ± 9.1 and was significantly higher than that of the *IL2RG* KO pigs (2.0 ± 1.4) (Fig. 2B' and C). Lymphocyte markers were verified by positive immunostaining (Fig. 3B–F). CD56+ cells were not abundant; however, numerous lymphoid cells infiltrated the transplanted tissue. CD3+ cells were strongly positive and many HLA-DR + cells were also identified (Fig. 3G). This indicates that lymphocytes were activated and that pigs with intact immune systems rejected the transplanted cells at the transplantation site. These phenomena were confirmed at all transplantation sites in all WT pigs.

In *IL2RG* KO pigs, the presence of tumors was confirmed 3 weeks after transplantation. There was a focal, moderately demarcated area composed of nests and packets of transplanted cells within the subcutis of the ears. Scarce lymphoid-related markers were detected in all transplanted sites (Fig. 4B–F). HLA-DR + cells were not detected (Fig. 4G), indicating that the immune system, including lymphocytes, was not activated and that there was no rejection or expansion of the transplanted cells at the transplanted site.

3.2.2. Experiment 2: evaluation of human cells transplanted into the pancreas of DPF IL2RG KO pigs housed in novel biocontainment facilities

The average body weight of the pigs did not differ significantly from that of the *IL2RG* KO pigs under conventional rearing. At 3 and 4 weeks post-transplantation (446–4 and 446–2, respectively), each pig was euthanized and the transplanted cells were confirmed (Fig. 5A and B). The tumors consisted of transplanted cells and strongly emitted red under fluorescent light (Fig. 5A and B, lower panels). The presence of a tumor with central necrosis was verified by HE staining (Fig. 5C, upper). At 3 and 4 weeks after transplantation, a small number of CD45+ cells were observed at the tumor boundary, but they did not infiltrate the tumor (Fig. 5C, lower, 446–4). Additionally, after the rearing period, swab samples were negative for bacteria, fungi, and protozoa (Table 1).

3.2.3. Experiment 3: comparison between the IL2RG KO pigs and other immunodeficient models

Operations to induce immunodeficiency were performed without complications, including infections and liver or renal dysfunction after transplantation (Suppl. Table 1). The weight gain was unstable in two pigs (Fig. 6A, K302 and K304). The transplanted cells were verified by red tdTomato color using a fluorescent lamp and filter (Fig. 6B–D). In two pigs, K302 and K304, red signals were observed at 2 weeks after transplantation (Fig. 6B and D); however, the body weights of these two pigs did not increase from day 3 after transplantation (Fig. 6A). The K303 pig did not have a visible tumor at 1 week post-transplantation (Fig. 6C) but showed healthy bodyweight gains (Fig. 6A). This pig did not reach the therapeutic effective blood concentration level of MMF from day 0–2 weeks post-transplantation (Supplementary Fig. 3).

4. Discussion

We have described the successful formation of human HeLa S3 cells in *IL2RG* KO pigs under several conditions. Pig models are highly effective and are employed for a plethora of translational medical research. SCID-like pigs, for example, comprise two independent mutations in the Artemis gene, which is a critical component of the V(D)J recombination pathway required for T and

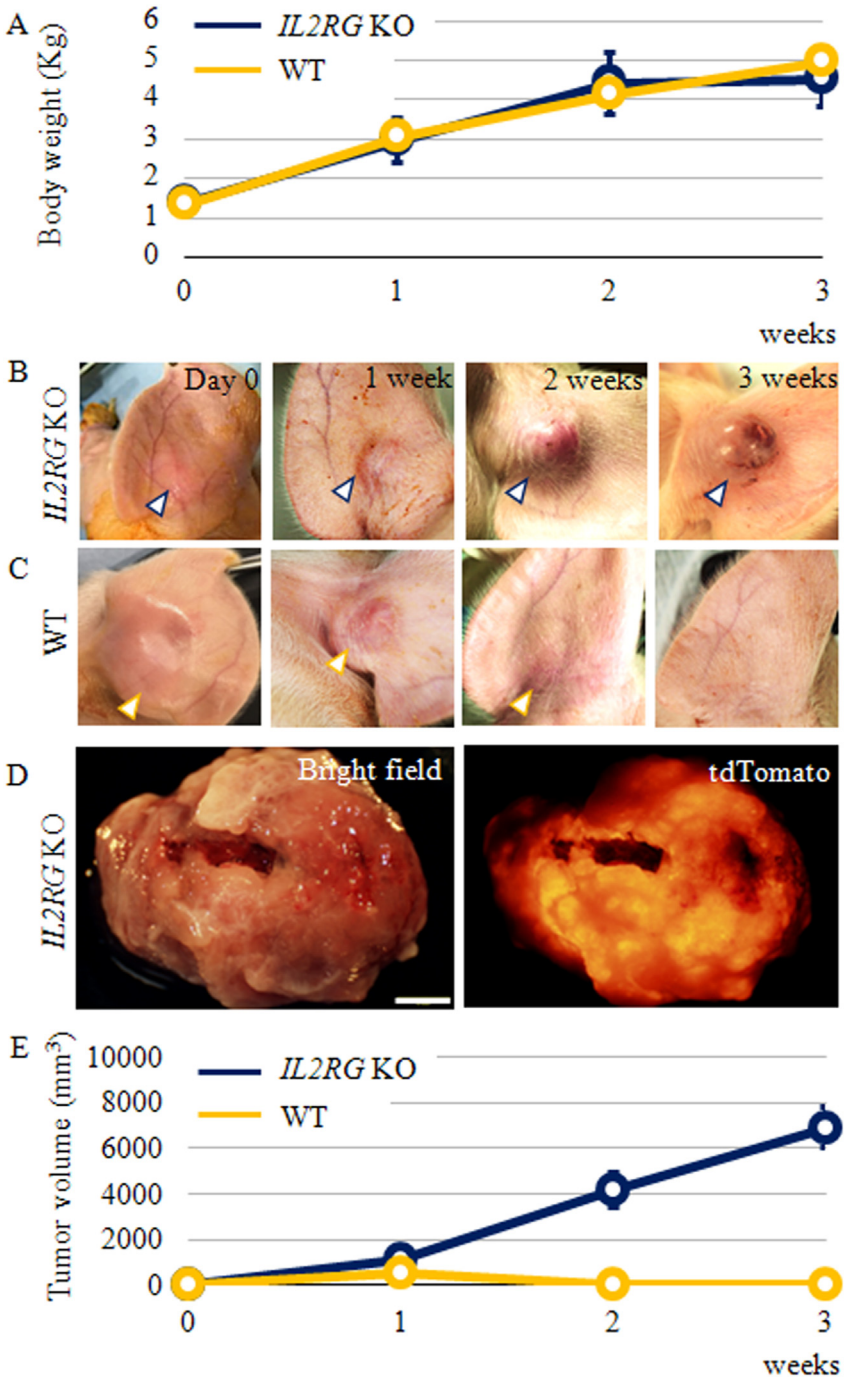

Fig. 1. Transplantation of HeLa S3 cells into subcutis of the ear in *IL2RG* KO and WT pigs. (A) Body weight gain of pigs over time. No differences were observed in the growth curves between the two groups. Blue line: *IL2RG* KO pigs (n = 7); Green line: WT pigs (n = 6). (B, C) Transplanted cells were monitored for tumor development. Photographs show an external view of tumor growth in the ear. (B) *IL2RG* KO pigs. Tumors derived from transplanted cells were identifiable in pig ears and their size increased with time. (C) WT pigs. Palpable tumors were observed in the ears of pigs 1 week after transplantation; however, no obvious tumors were observed at the transplantation site from 2 weeks after transplantation. (D) Broad photograph of the dissected tumor derived from an *IL2RG* KO pig. For the donor cells in this study, we selected the HeLa S3 cell line, which was modified to express tdTomato. The tumor was inspected with a fluorescent lamp and filter to verify whether the tumor emitted tdTomato. (D, left) Bright-field stereomicroscopic images of dissected tumors at 3 weeks after transplantation. (D, right) Fluorescence-stereomicroscopic image (left panel). The tumor exhibited a strong red signal. Scale bar: 5 mm. (E) Tumor volume in both groups. Two *IL2RG* KO pigs and three WT pigs received cell transplants in both ears, while all others received them in one ear only. Blue line: *IL2RG* KO pigs (n = 9); Green line: WT pigs (n = 9). The time after birth is indicated as weeks. Quantitative data are presented as mean ± SD.

B cell receptor development. The pigs have a T^- B– NK^+ cellular phenotype [26]. One drawback of this model is that the NK cells in the pigs are functional [47], which could have antitumor activity in human cancer cells [31]. Another model, the *RAG2* KO pig, has been used for studies on human cell xenotransplantation [32,33]. Although the pigs also had a T^- B– NK^+ cellular phenotype, they did not reject iPS cell lines or porcine cells with a trophoblast phenotype [33]. Our SCID-like model, the *IL2RG* KO pig, is similar to human X-linked SCID patients with a T^- B^+ NK^- cellular phenotype [23]; however, the ability to obtain large numbers of these

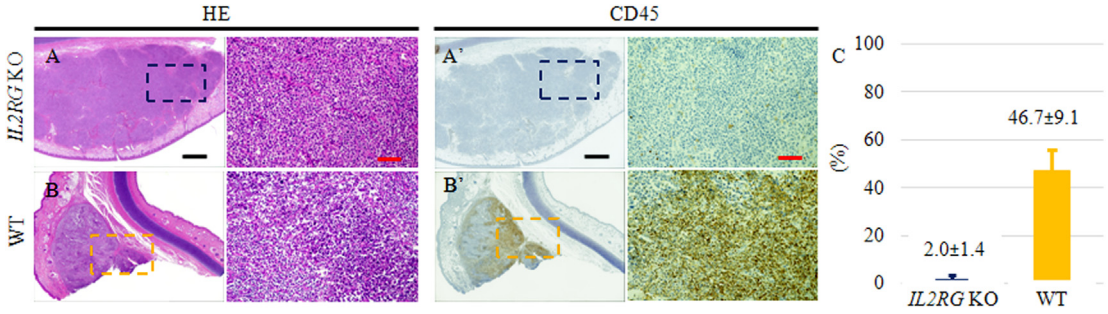

Fig. 2. Histological evaluation of tumors within the subcutis of the ear of pigs at 1 week after transplantation. (A, A′) *IL2RG* KO pigs. (B, B′) WT pigs. (A) HE staining. Tumors were visible, well demarcated, and formed nests in the ears (A, left). The transplanted cells expanded clonally at the transplantation site (A, right). (A′) CD45 staining. Scarce CD45+ cells were detected in the tumor. (B) HE staining. Within the subcutis of the ears of WT pigs, there were moderately demarcated tumors (B, left); however, they were not as dense as the tumors of *IL2RG* KO pigs (B, right). (B′) CD45 staining. CD45+ cells were evident and abundant within the tumor. Scale bars: black, 10 mm; red, 100 μm. (C) Lymphocyte infiltration. The number of CD45+ lymphocytes was counted and compared between the *IL2RG* KO and WT groups as the rate of CD45+ lymphocytes in the tumor area. In WT pigs, CD45+ cells comprised 46.7% of the tumor area, which was significantly higher than that in the *IL2RG* KO pigs (*$p < 0.05$). Data are presented as the mean ± SD of six independent experiments.

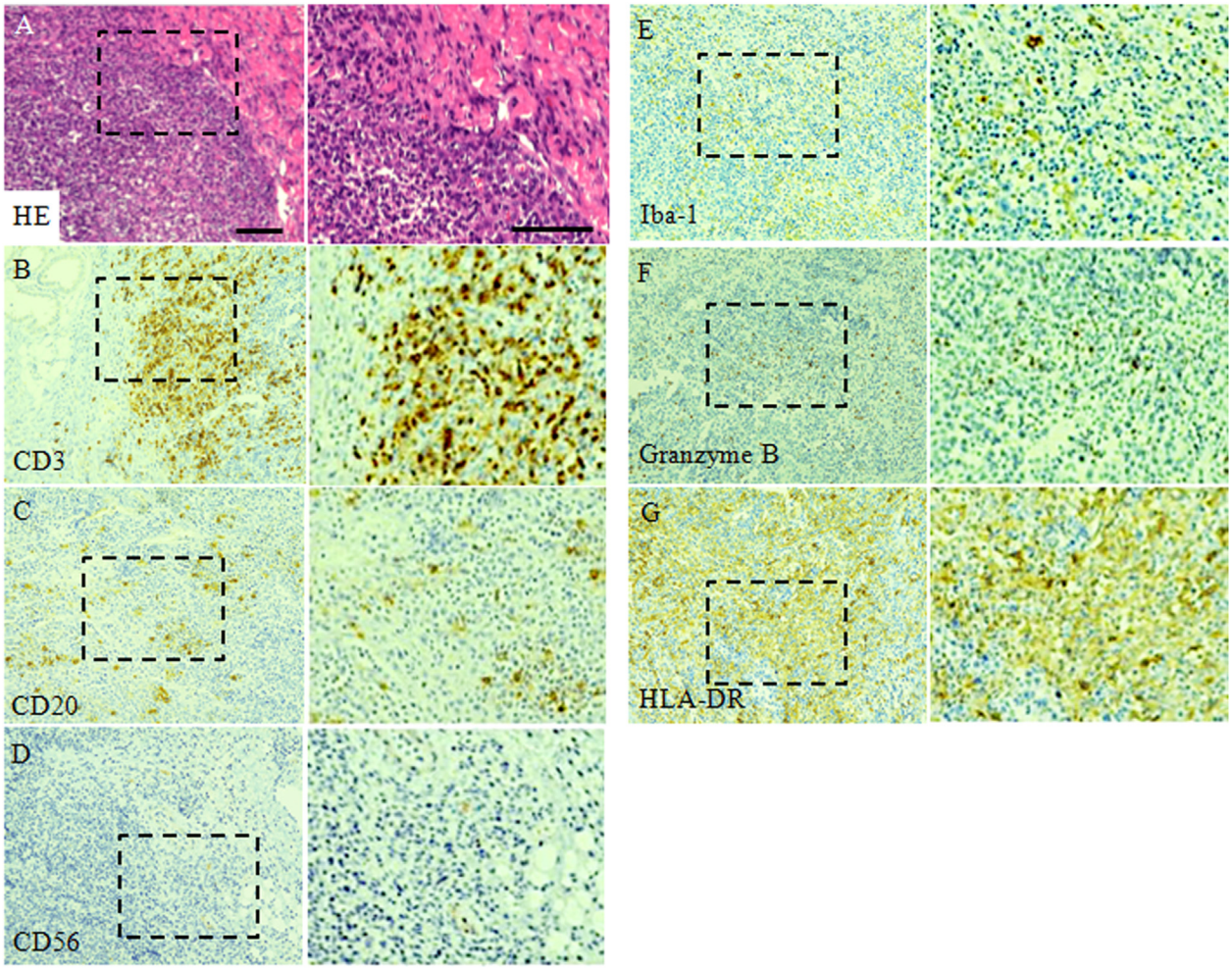

Fig. 3. Histological analysis of the transplanted cells in WT pigs 1 week after transplantation. (A–G) Tumors derived from transplanted cells within the subcutis of the ear. The right panels show an enlarged image of each stain. (A) HE staining. Moderately encapsulated and infiltrative tumors were visible. (B–F) Lymphocyte markers were verified by immunostaining. (B) T lymphocyte marker, CD3. (C) B lymphocyte marker, CD20. (D) NK cell marker, CD56. (E) Monocyte/macrophage lineage and dendritic cell marker, Iba1. (F) Cytotoxic T cell and NK cell marker, granzyme B. (G) Major histocompatibility complex class II molecule marker, HLA-DR. Numerous lymphoid cells infiltrated the tumor and lymphocyte activation was confirmed; therefore, rejection of transplanted cells by pigs with an intact immune system occurred at the transplantation site. These phenomena were confirmed in all WT pigs. Scale bar: 100 μm.

genetically engineered animals is greatly limited by expense. Additionally, the use of this model is associated with other critical issues. X-linked SCID patients typically die from severe infections in the first year of life if they do not receive any treatment [48–50]. We found that *IL2RG* KO pigs were also prone to systemic infection and suffered from severe complex infections by three weeks after birth under conventional housing conditions [25]. Furthermore, the generation of cloned gene KO pigs via SCNT is prone to be

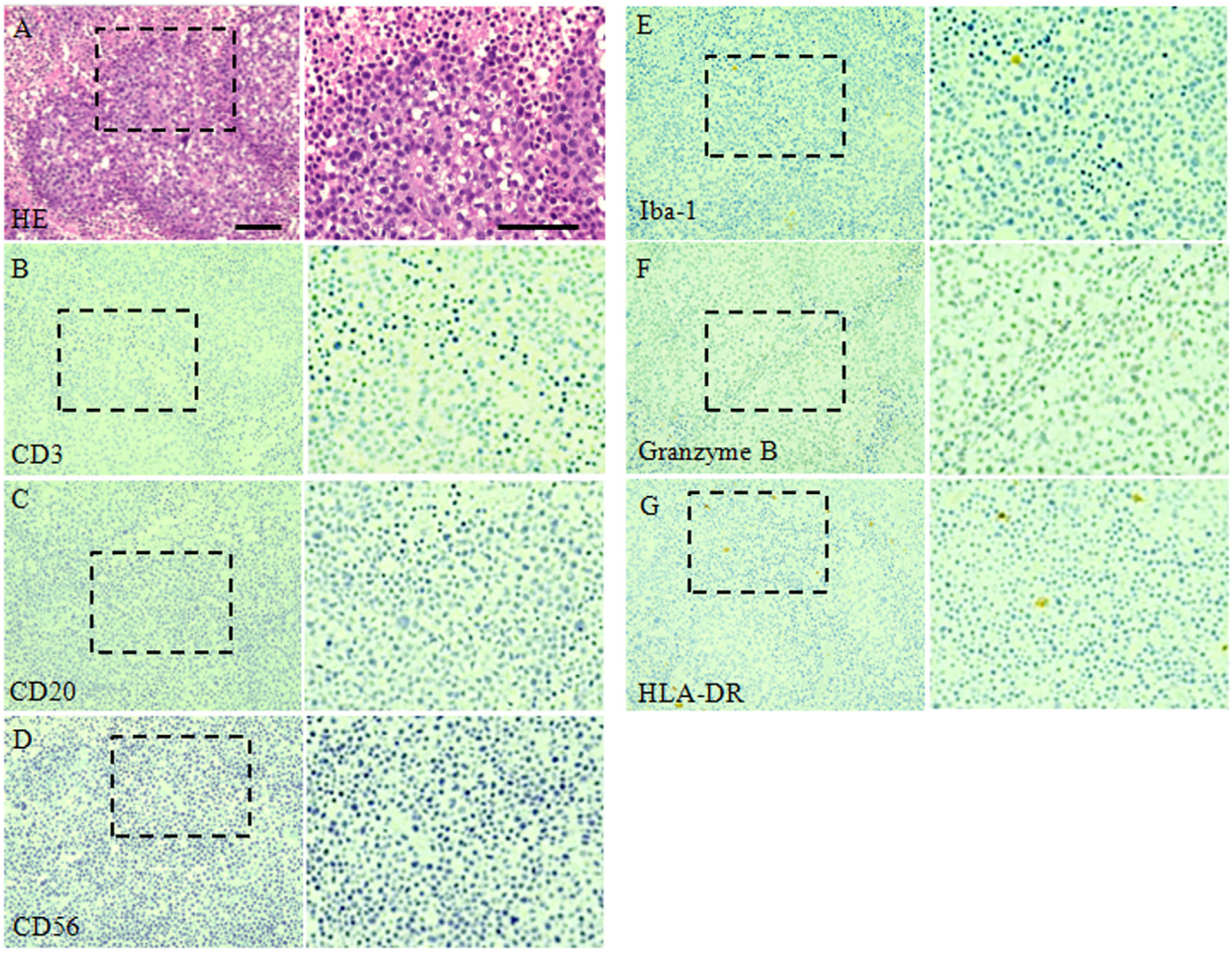

Fig. 4. Histological analysis of the transplanted cells in *IL2RG* KO pigs 3 weeks after transplantation. (A–G) Tumors derived from transplanted cells within the subcutis of the ears. The right panels show the enlargement of each staining. (A) HE staining. There is a focal, moderately demarcated area composed of nests and packets of transplanted cells within the subcutis of the ears. (B–F) Lymphocyte markers were verified by immunostaining. (B) T lymphocyte marker, CD3. (C) B lymphocyte marker, CD20. (D) NK cell marker, CD56. (E) Monocyte/macrophage lineage and dendritic cell marker, Iba1. (F) Cytotoxic T cell and NK cell marker, granzyme B. (G) Major histocompatibility complex class II molecule marker, HLA-DR. In *IL2RG* KO pigs, scarce lymphoid-related markers were confirmed at all transplanted sites. The transplanted cells were not rejected and formed tumors at the transplanted sites. Scale bar: 100 μm.

influenced by epigenetic dysregulation [51]. Thus, it is difficult to generate healthy, fertile boars and these hurdles should be carefully considered when implementing the *IL2RG* KO pig model in future studies.

Rescue experiments on embryos carrying lethal genetic mutations through chimerism with normal cells have given rise to individuals with normalized traits [52–54]. In our previous study, we generated chimeric boars composed of *IL2RG* KO cells and normal cells, because SCID is an X-linked disease. The chimeric boars exhibited a cured fertile phenotype while carrying and transmitting the SCID-like genotype. They appeared physiologically normal and remained healthy until up to 3 years of age under conventional rearing conditions [25]. This allowed for the routine production of *IL2RG* KO pigs through male-based breeding. All *IL2RG* KO pigs utilized in this study had a healthy reproductive system.

In the current study, we investigated whether human cells could ectopically develop tumors in *IL2RG* KO pigs. The transplanted cells developed in all of our SCID-like pigs and lymphatic markers were negative for the transplanted cells. Preliminary results indicated that B lymphocytes were present in *IL2RG* KO pigs, but disappeared by 12 weeks after birth [23,36]. It is known that B cells need T cell-associated cytokine stimulation to be functional [55,56]. In this study, CD3, CD8, CD45+, and the B cell marker CD20+ cells were not confirmed 3 weeks after transplantation, suggesting that B cells were not functional at the transplanted sites. Killer T cells were also not produced due to the negative expression of lba1 and granzyme B. We focused on the analysis of human cells in the present study because we plan to develop a human cancer study using *IL2RG* KO pigs in the near future. However, the pigs have also been previously engrafted with non-cancer cells; mouse whole pancreases were transplanted into the omentum. The transplanted pancreatic cells were also confirmed at 14 days after transplantation (data not shown).

These results may indicate support of the immune system in *IL2RG* KO pigs, because lymphocytes, including B cells, are not functional in the early stages of their lives.

For Experiment 1, we chose an easily monitored tumor location, in the ears of pigs. However, we will explore more challenging cancer studies in the future, especially pancreatic cancer, using orthotopic models. Pancreatic cancer, a particularly devastating human cancer, should be explored in pig models to determine their suitability. One of the major problems with current animal models of human tumors is their low translatability to clinical settings [31]. Once a pig tumor model is generated with *IL2RG* KO pigs, it could be

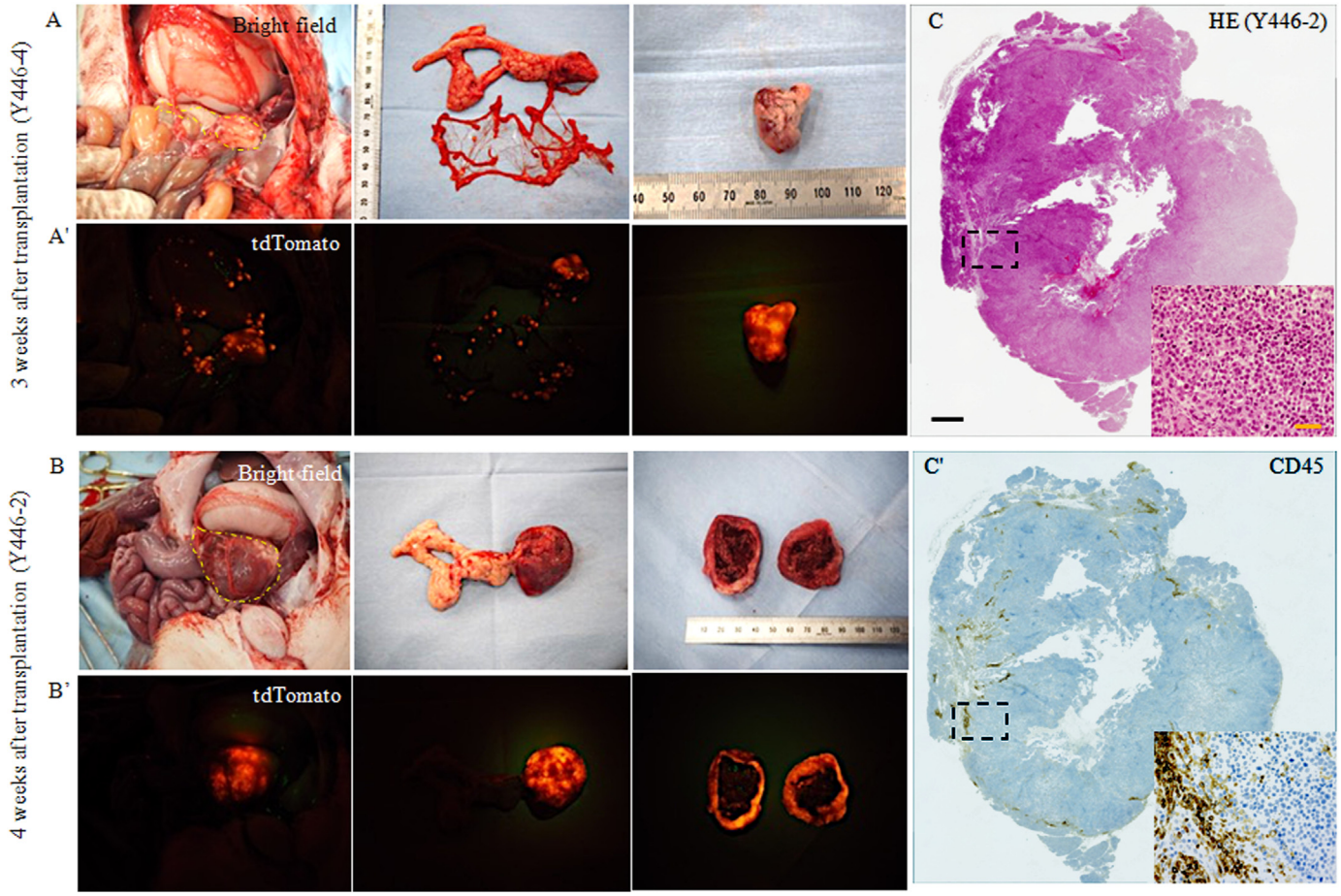

Fig. 5. Transplantation of HeLa S3 cells into the pancreas of DPF *IL2RG* KO pigs. Two 7-day-old *IL2RG* KO pigs underwent laparotomy in an isolator unit under sterile conditions. tdTomato-expressing HeLa S3 cells were transplanted into the tail of the pancreas in the pigs. (A and B) Broad bright-field photographs of tumors at 3 (Y446-4) and 4 weeks (Y446-2) after transplantation. (A and B, left panels) Macroscopic appearance of the pancreas. The yellow lines show the outline of each pancreas. (A and B, middle panels) Macroscopic appearance of a dissected pancreas. A large tumor was observed in the pancreatic tail. (A and B, right panels) Dissected tumors. (A′ and B′) Fluorescence-stereomicroscopic image of the tumor in *IL2RG* KO pigs. The tumor was inspected with a fluorescent lamp and filter to verify whether it emitted tdTomato. The transplanted cells in the pancreas appeared bright red. (A′ and B′, left and middle panels). The dissected tumor exhibited a strong red signal (A′ and B′, right panels). (C, C′) Histological appearance of a tumor (Y446-4). The tumor was HE stained and labeled with CD45. Each right lower panel is an enlargement of the images in C and C′. C and C′ are lower magnifications of the dissected tumor. (B) HE staining. The tumors exhibited central necrosis. (C′) A small number of CD45+ cells were verified at the boundary of the tumor, but they did not infiltrate. The time after birth is indicated weeks. Scale bars: black = 10 mm; yellow = 100 μm.

Table 1
Microbiological testing.

No	sample	0 weeks			3 weeks			4 weeks		
		aerobic bacteria	anaerobic bacteria	fungi	aerobic bacteria	anaerobic bacteria	fungi	aerobic bacteria	anaerobic bacteria	fungi
Y446-4	oral mucosa	–	–	–	–	–	–			
	Skin	–	–	–	–	–	–			
	Stool	–	–	–	–	–	–			
Y446-2	oral mucosa	–	–	–	NT	NT	NT	–	–	–
	Skin	–	–	–				–	–	–
	Stool	–	–	–				–	–	–
Isolator	Isolator	–	–	–	–	–	–	–	–	–

NT; Not tested.
For DPF pigs produced using the U-iR method, swab samples of the body surface, the oral mucosa, the feces, and the internal surface of the rearing unit were collected weekly during the study. The samples were cultured on thioglycolate and potato dextrose agar and examined using a standard protocol developed and recommended by the Japanese Association for Laboratory Animal Science.

chiefly employed for testing chemotherapy, radiotherapy, and surgical reduction strategies with more realistic results. To elucidate the effectiveness of anticancer treatments, studies require long-term follow-up. Therefore, pigs should be maintained in an environment where pathogen exposure is minimized and the risk of premature death due to SCID-related complications is reduced. Thus, establishing an efficient system to produce DPF pigs is essential for studies of this nature.

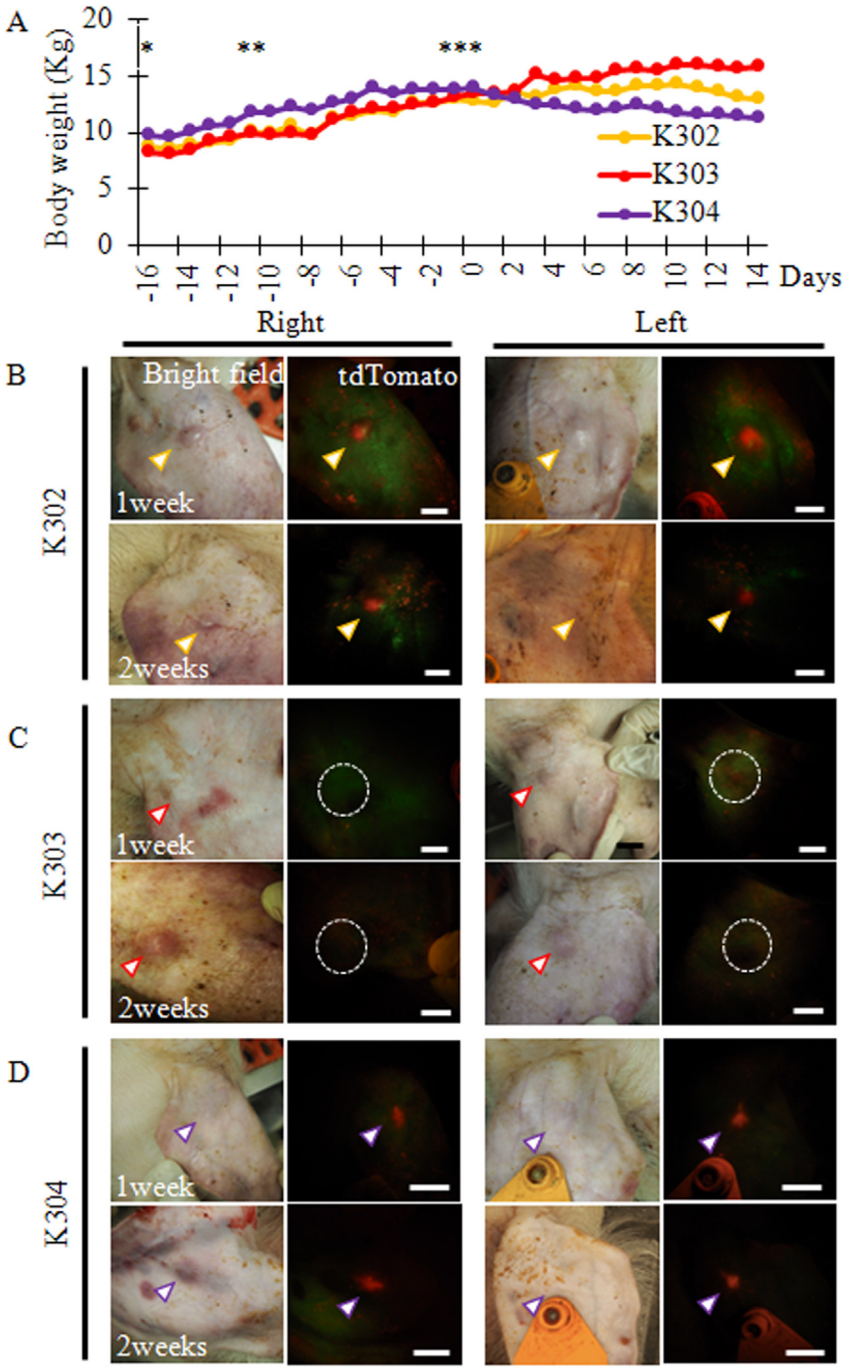

Fig. 6. Comparison between *IL2RG* KO pigs and other immunodeficient models. Three different immunodeficient pigs were produced by the following operations: K302 underwent thymectomy, splenectomy, and gastrostomy. K303 underwent thymectomy and gastrostomy. K304 underwent gastrostomy. (A) Body weights at specified times. The body weight gain was unstable in two pigs after transplantation (K302 and K304). Yellow line: K302; red line: K303; purple line: K304. The time after birth is indicated as days and weeks. * Production of different immunodeficient pigs, ** Treated with immunosuppressive drugs, *** Transplantation. (B–D) The transplanted cells were verified by the red tdTomato color at the transplanted sites using a fluorescent lamp and filter. In two pigs, K302 and K304, red signals were observed 2 weeks after transplantation. No tumor was identified in the ears of K303 at 1 week post-transplantation. Scale bar: 10 mm.

In Experiment 2, human cells were transplanted into the pancreas of *IL2RG* KO pigs under aseptic conditions. The fluorescent marker tdTomato was used to identify HeLa S3 cells, which were traceable by human-specific imaging systems, even outside the pig's body. We attempted this study with a prototype of a small isolator unit; hence, we were limited to a maximum study length of 5 weeks, after which the pigs would be too large. We are in the process of constructing a larger unit, which will allow us to perform long-term follow-up studies. Ultimately, we confirmed that human cells could successfully develop in the pancreas of *IL2RG* pigs, providing a basis for the refinement of a pancreatic cancer model in pigs. We have subsequently commenced further pancreatic cancer studies on human pancreatic cell lines in *IL2RG* KO pigs.

This study also comparatively investigated whether *IL2RG* KO pigs are superior xenotransplantation models to other immunodeficient models, in Experiment 3. In WT pigs, the blood

concentrations of immunosuppressive drugs fluctuate according to their dosage, making it difficult to uniformly induce immunodeficiency. All three pigs in this experiment exceeded the therapeutic range of tacrolimus, while two of them exhibited lower therapeutic levels of MMF after transplantation. Furthermore, we used neonatal WT animals because of their quick development and, consequently, immunosuppressive drugs could not be monitored promptly. Indeed, the drug concentration levels of MMF for K302 and K303 were not within the therapeutic range, even when administered according to the protocol [35]. The therapeutic range for neonatal pigs was narrow due to their light body weight and, as such, the concentration of tacrolimus was much higher. In addition, the timing of immunosuppressive drug monitoring is critical and, in our study, the results could only be returned with a 3–4 day delay. Thus, without knowing the blood concentration levels of drugs on a daily basis, such as in human organ transplantation, it was difficult to control the concentration within the expected ranges.

5. Conclusions

We demonstrate that *IL2RG* KO pigs could be an effective host for human cells and that pig models should be further explored in various biomedical fields, such as stem cell, cancer, and translational research.

Declaration of competing interest

The authors have no conflicts of interest.

Acknowledgments

We thank Dr. Erica Furukawa for technical assistance. This research work was supported by Grants-in-Aid from the Ministry of Education, Culture, Sports, Science, and Technology of Japan (20K08944 to M.N.); the Japan Agency for Medical Research and Development (Leading Advanced Projects for Medical Innovation [LEAP]; the Generation of Functional Organs using Developmental Niche (to H. N); the Japan Science and Technology Agency (Exploratory Research for Advanced Technology [ERATO]; NAKAUCHI Stem Cell and Organ Regeneration (to H. N.); and the Meiji University International Institute for Bio-Resource Research (to H.N). The funding organizations played no role in the study's design, data collection and analysis, the decision to publish, or the manuscript's preparation.

Appendix A. Supplementary data

Supplementary data to this article can be found online at https://doi.org/10.1016/j.reth.2022.05.010.

References

[1] Caldwell J. The current status of attempts to predict species differences in drug metabolism. Drug Metab Rev 1981;12:221–37.
[2] Bogaards JJ, Bertrand M, Jackson P, Oudshoorn MJ, Weaver RJ, van Bladeren PJ, et al. Determining the best animal model for human cytochrome P450 activities: a comparison of mouse, rat, rabbit, dog, micropig, monkey and man. Xenobiotica 2000;30:1131–52.
[3] Trobridge GD, Kiem HP. Large animal models of hematopoietic stem cell gene therapy. Gene Ther 2010;17:939–48.
[4] Dalgaard L. Comparison of minipig, dog, monkey and human drug metabolism and disposition. J Pharmacol Toxicol Methods 2015;74:80–92.
[5] Swanson KS, Mazur MJ, Vashisht K, Rund LA, Beever JE, Counter CM, et al. Genomics and clinical medicine: rationale for creating and effectively evaluating animal models. Exp Biol Med 2004;229:866–75.
[6] Meurens F, Summerfield A, Nauwynck H, Saif L, Gerdts V. The pig: a model for human infectious diseases. Trends Microbiol 2012;20:50–7.
[7] Walters EM, Prather RS. Advancing swine models for human health and diseases. Mo Med 2013;110:212–5.
[8] Asao H, Okuyama C, Kumaki S, Ishii N, Tsuchiya S, Foster D, et al. Cutting edge: the common γ-chain is an indispensable subunit of the IL-21 receptor complex. J Immunol 2001;167:1–5.
[9] Giri JG, Ahdieh M, Eisenman J, Shanebeck K, Grabstein K, Kumaki S, et al. Utilization of the β and γ chains of the IL-2 receptor by the novel cytokine IL-15. EMBO J 1994;13:2822–30.
[10] Kimura Y, Takeshita T, Kondo M, Ishii N, Nakamura M, Van Snick J, et al. Sharing of the IL-2 receptor γ chain with the functional IL-9 receptor complex. Int Immunol 1995;7:115–20.
[11] Kondo M, Takeshita T, Ishii N, Nakamura M, Watanabe S, Arai KI, et al. Sharing of the interleukin-2 (IL-2) receptor γ chain between receptors for IL-2 and IL-4. Science 1993;262:1874–7.
[12] Noguchi M, Nakamura Y, Russell SM, Ziegler SF, Tsang M, Cao X, et al. Interleukin-2 receptor γ chain: a functional component of the interleukin-7 receptor. Science 1993;262:1877–80.
[13] Noguchi M, Yi H, Rosenblatt HM, Filipovich AH, Adelstein S, Modi WS, et al. Interleukin-2 receptor γ chain mutation results in X-linked severe combined immunodeficiency in humans. Cell 1993;73:147–57.
[14] Russell SM, Keegan AD, Harada N, Nakamura Y, Noguchi M, Leland P, et al. Interleukin-2 receptor gamma chain: a functional component of the interleukin-4 receptor. Science 1993;262:1880–3.
[15] Honma D, Uenishi H, Hiraiwa H, Watanabe S, Tang W, Kiyokawa N, et al. Cloning and characterization of porcine common γ chain gene. J Interferon Cytokine Res 2003;23:101–11.
[16] Ishii N, Takeshita T, Kimura Y, Tada K, Kondo M, Nakamura M, et al. Expression of the IL-2 receptor γ chain on various populations in human peripheral blood. Int Immunol 1994;6:1273–7.
[17] Minegishi M, Tsuchiya S, Imaizumi M, Yamaguchi Y, Goto Y, Tamura M, et al. Successful transplantation of soy bean agglutinin-fractionated, histoincompatible, maternal marrow in a patient with severe combined immunodeficiency and BCG infection. Eur J Pediatr 1985;143:291–4.
[18] Bosma GC, Custer RP, Bosma MJ. A severe combined immunodeficiency mutation in the mouse. Nature 1983;301:527–30.
[19] Mestas J, Hughes CC. Of mice and not men: differences between mouse and human immunology. J Immunol 2004;172:2731–8.
[20] Basel MT, Balivada S, Beck AP, Kerrigan MA, Pyle MM, Dekkers JC, et al. Human xenografts are not rejected in a naturally occurring immunodeficient porcine line: a human tumor model in pigs. Biores Open Access 2012;1:63–8.
[21] Ozuna AG, Rowland RR, Nietfeld JC, Kerrigan MA, Dekkers JC, Wyatt CR. Preliminary findings of a previously unrecognized porcine primary immunodeficiency disorder. Vet Pathol 2013;50:144–6.
[22] Suzuki S, Iwamoto M, Saito Y, Fuchimoto D, Sembon S, Suzuki M, et al. IL2RG gene-targeted severe combined immunodeficiency pigs. Cell Stem Cell 2012;10:753–8.
[23] Watanabe M, Nakano K, Matsunari H, Matsuda T, Maehara M, Kanai K, et al. Generation of interleukin-2 receptor gamma gene knockout pigs from somatic cells genetically modified by zinc finger nuclease-encoding mRNA. PLoS One 2013;8:e76478.
[24] Hauschild J, Petersen B, Santiago Y, Queisser AL, Carnwath JW, Lucas-Hahn A, et al. Efficient generation of a biallelic knockout in pigs using zinc- finger nucleases. Proc Natl Acad Sci U S A 2011;108:12013–7.
[25] Matsunari H, Watanabe M, Nakano K, Enosawa S, Umeyama K, Uchikura A, et al. Modeling lethal X-linked genetic disorders in pigs with ensured fertility. Proc Natl Acad Sci U S A 2018;115:708–13.
[26] Waide EH, Dekkers JCM, Ross JW, Rowland RRR, Wyatt CR, Ewen CL, et al. Not all SCID pigs are created equally: two independent mutations in the Artemis gene cause SCID in pigs. J Immunol 2015;195:3171–9.
[27] Kang J-T, Cho B, Ryu J, Ray C, Lee E-J, Yun Y-J, et al. Biallelic modification of IL2RG leads to severe combined immunodeficiency in pigs. Reprod Biol Endocrinol 2016;14:74.
[28] Huang J, Guo X, Fan N, Song J, Zhao B, Ouyang Z, et al. RAG1/2 knockout pigs with severe combined immunodeficiency. J Immunol 2014;193:1496–503.
[29] Ito T, Sendai Y, Yamazaki S, Seki-Soma M, Hirose K, Watanabe M, et al. Generation of recombination activating gene-1-deficient neonatal piglets: a model of T and B cell deficient severe combined immune deficiency. PLoS One 2014;9:e113833.
[30] Boettcher AN, Loving CL, Cunnick JE, Tuggle CK. Development of severe combined immunodeficient (SCID) pig models for translational cancer modeling: future insights on how humanized SCID pigs can improve preclinical cancer research. Front Oncol 2018;8:559.
[31] Boettcher AN, Kiupel M, Adur MK, Cocco E, Santin AD, Bellone S, et al. Human ovarian cancer tumor formation in severe combined immunodeficient (SCID) pigs. Front Oncol 2019;9:9.
[32] Choi YJ, Kim E, Reza AMMT, Hong K, Song H, Park C, et al. Recombination activating gene-2^{null} severe combined immunodeficient pigs and mice engraft human induced pluripotent stem cells differently. Oncotarget 2017;8:69398–407.
[33] Lee K, Kwon DN, Ezashi T, Choi YJ, Park C, Ericsson AC, et al. Engraftment of human iPS cells and allogeneic porcine cells into pigs with inactivated RAG2 and accompanying severe combined immunodeficiency. Proc Natl Acad Sci U S A 2014;111:7260–5.

[34] Nakano K, Hasegawa K, Inoue R, Yamada T, Ebisutani R, Hiraide K, et al. Production of medical grade pigs using the uterectomy-isolated rearing (U-iR) method. Xenotransplantation 2019;26:e75.
[35] Itoh M, Mukae Y, Kitsuka T, Arai K, Nakamura A, Uchihashi K, et al. Development of an immunodeficient pig model allowing long-term accommodation of artificial human vascular tubes. Nat Commun 2019;10:2244.
[36] Hara H, Shibata H, Nakano K, Abe T, Uosaki H, Ohnuki T, et al. Production and rearing of germ-free X-SCID pigs. Exp Anim 2018;67:139–46.
[37] Maejima K, Nomura T. An experience of application of sterility test of germ-free mice and rats recommended by JEARA. Jikken Dobutsu 1975;24:177–81 (Japanese).
[38] Watanabe M, Kobayashi M, Nagaya M, Matsunari H, Nakano K, Maehara M, et al. Production of transgenic cloned pigs expressing the far-red fluorescent protein monomeric Plum. J Reprod Dev 2015;61:169–77.
[39] Nagaya M, Katsumata Y, Arai Y, Umeki I, Nakano K, Kasai Y, et al. Effectiveness of bioengineered islet cell sheets for the treatment of diabetes mellitus. J Surg Res 2018;227:119–29.
[40] Nagaya M, Hayashi A, Nakano K, Honda M, Hasegawa K, Okamoto K, et al. Distributions of endocrine cell clusters during porcine pancreatic development. PLoS One 2019;14:e0216254.
[41] Poli A, Michel T, Thérésine M, Andrès E, Hentges F, Zimmer J. CD56bright natural killer (NK) cells: an important NK cell subset. Immunology 2009;126:458–65.
[42] Pierezan F, Mansell J, Ambrus A, Rodrigues Hoffmann A. Immunohistochemical expression of ionized calcium binding adapter molecule 1 in cutaneous histiocytic proliferative, neoplastic and inflammatory disorders of dogs and cats. J Comp Pathol 2014;151:347–51.
[43] Huang A, Shinde PV, Huang J, Senff T, Xu HC, Margotta C, et al. Progranulin prevents regulatory NK cell cytotoxicity against antiviral T cells. JCI Insight 2019;4:e129856.
[44] Luo ZW, Xia K, Liu YW, Liu JH, Rao SS, Hu XK, et al. Extracellular vesicles from akkermansia muciniphila elicit antitumor immunity against prostate cancer via modulation of $CD8^+$ T cells and macrophages. Int J Nanomed 2021;16:2949–63.
[45] Naziruddin B, Durriya S, Phelan D, Duffy BF, Olack B, Smith D, et al. HLA antibodies present in the sera of sensitized patients awaiting renal transplant are also reactive to swine leukocyte antigens. Transplantation 1998;66:1074–80.
[46] Díaz Varela I, Sánchez Mozo P, Centeno Cortés A, Alonso Blanco C, Valdés Cañedo F. Cross-reactivity between swine leukocyte antigen and human anti-HLA-specific antibodies in sensitized patients awaiting renal transplantation. J Am Soc Nephrol 2003;14:2677–83.
[47] Powell EJ, Cunnick JE, Knetter SM, Loving CL, Waide EH, Dekkers JCM, et al. NK cells are intrinsically functional in pigs with Severe Combined Immunodeficiency (SCID) caused by spontaneous mutations in the Artemis gene. Vet Immunol Immunopathol 2016;175:1–6.
[48] Blanco E, Izotova N, Booth C, Thrasher AJ. Immune reconstitution after gene therapy approaches in patients with X-linked severe combined immunodeficiency disease. Front Immunol 2020;11:608653.
[49] Liao W, Lin JX, Leonard WJ. Interleukin-2 at the crossroads of effector responses, tolerance, and immunotherapy. Immunity 2013;38:13–25.
[50] Qasim W, Gaspar HB, Thrasher AJ. Gene therapy for severe combined immune deficiency. Expet Rev Mol Med 2004;6:1–15.
[51] Zhao J, Whyte J, Prather RS. Effect of epigenetic regulation during swine embryogenesis and on cloning by nuclear transfer. Cell Tissue Res 2010;341:13–21.
[52] Chen J, Lansford R, Stewart V, Young F, Alt FW. RAG-2-deficient blastocyst complementation: an assay of gene function in lymphocyte development. Proc Natl Acad Sci U S A 1993;90:4528–32.
[53] Kobayashi T, Yamaguchi T, Hamanaka S, Kato-Itoh M, Yamazaki Y, Ibata M, et al. Generation of rat pancreas in mouse by interspecific blastocyst injection of pluripotent stem cells. Cell 2010;142:787–99.
[54] Matsunari H, Nagashima H, Watanabe M, Umeyama K, Nakano K, Nagaya M, et al. Blastocyst complementation generates exogenic pancreas in vivo in apancreatic cloned pigs. Proc Natl Acad Sci U S A 2013;110:4557–62.
[55] Conley ME. Molecular approaches to analysis of X-linked immunodeficiencies. Annu Rev Immunol 1992;10:215–38.
[56] Gelfand EW, Dosch HM. Diagnosis and classification of severe combined immunodeficiency disease. Birth Defects Orig Artic Ser 1983;19:65–72.